

# Service Provisioning with Energy-Aware Regenerator Allocation in Multi-Domain EONs

Jing Zhu, Xiaoliang Chen, Di Chen, Shilin Zhu, Zuqing Zhu<sup>†</sup>

School of Information Science and Technology, University of Science and Technology of China, Hefei, China

<sup>†</sup>Email: {zqzhu}@ieee.org

**Abstract**—As multi-domain elastic optical networks (EONs) can enhance network scalability, extend service reach, and accommodate the inter-operability issues, it is very relevant to consider them in practical network operations. In this work, we study the problem of how to achieve energy-aware service provisioning in a multi-domain EON, where the optoelectronic regenerators only exist in border nodes. We consider dynamic lightpath requests and propose two algorithms, *i.e.*, the greedy regenerator allocation (GRA) and the set-cover based regenerator allocation (STC), to realize the joint optimization of routing, modulation and spectrum assignment (RMSA) and regenerator allocation. The algorithms are evaluated with extensive simulations that use multi-domain EONs built with different regenerator placement strategies. The results verify that GRA and STC outperform the existing algorithm for energy-aware multi-domain service provisioning, and STC achieves the best performance in terms of both blocking probability and power efficiency.

**Index Terms**—Multi-domain, Elastic optical networks (EONs), Energy-aware regenerator allocation

## I. INTRODUCTION

It is known that flexible-grid elastic optical networks (EONs) allow network operators to manage optical spectra more adaptively without being constrained by the fixed spectral grids [1]. Specifically, by leveraging advanced optical transmission and switching technologies, EONs provide a spectrum allocation granularity at 12.5 GHz or less and support super-channels with more than 400 GHz bandwidth as well. Hence, EONs are more promising than the fixed-grid wavelength-division multiplexing (WDM) networks for future optical networks.

When the world-wide deployment of EONs takes place, multi-domain scenarios have to be incorporated [2]. In addition to enhancing network scalability and extending service reach, multi-domain service provisioning can accommodate the inter-operability issues when network elements from different vendors have to be used, and handle the situation in which optical nodes are geographically distributed and/or operated by different carriers. As optical signals will become more degraded after longer fiber transmission, the quality of transmission (QoT) has to be carefully considered in multi-domain EONs. To successfully provision a lightpath across multiple domains, we need to use optoelectronic regenerator(s) when the transmission distance exceeds the maximum reach under certain QoT constraint. Meanwhile, in EONs, one can use distance-adaptive modulation selection for supporting different transmission distances [3, 4]. Even though a higher modulation-level can bring in higher spectrum efficiency, the maximum transmission reach also decreases dramatically

due to the lower receiver sensitivity [3]. Consequently, more regenerators will be required, which pushes up the energy consumption. Therefore, we need to consider energy-aware regenerator allocation for the service provisioning in multi-domain EONs and balance the tradeoff between energy-consumption and spectrum efficiency.

Previously, people have investigated the problem of regenerator allocation and routing and wavelength assignment (RWA) in translucent WDM networks [5–9]. However, the schemes proposed in them cannot address the unique features of EONs, *e.g.*, flexible spectrum allocation and distance-adaptive modulation selection, and hence are not suitable for EONs. For static network planning, recent studies have considered the problem of regenerator placement in translucent EONs [10–12]. In [10], the author verified that the spectrum utilization in an EON can be reduced considerably by introducing regenerators. Cerutti *et al.* tried to optimize the routing, modulation and spectrum assignment (RMSA) and regenerator placement jointly in EONs and proposed a genetic algorithm (GA) based approach to minimize the regeneration nodes and spectrum utilization [11]. However, it is known that GA-based approaches usually take relatively long computation time and hence may not be suitable for online provisioning. In [12], the energy consumption of translucent EONs has been considered and an energy-efficient routing and spectrum assignment (RSA) algorithm with selective regenerator placement was developed. However, the energy model in [12] assumed that the modulation format of a lightpath would not change end-to-end, which did not fully explore the flexibility of regenerators in EONs. Note that the studies in [10–12] were for regenerator placement and assumed that an optoelectronic regenerator can be placed anywhere in an EON. Nevertheless, this may not be the case in multi-domain EONs. For instance, operators may only allow the border nodes to become regeneration sites for achieving inter-operation among domains as well as cost-saving.

The dynamic service provisioning in translucent EONs has been addressed in [13], where several impairment-aware service provisioning algorithms were proposed for load balancing. Specifically, the authors utilized a layered auxiliary graph to determine the RMSA and regenerator allocation for each lightpath. However, they did not try to balance the tradeoff between the energy-consumption of regenerators and spectrum efficiency. Moreover, the auxiliary graph can become really complex for a multi-domain EON with a relatively large topology and many feasible modulation formats, which make

the proposed scheme not scale well.

In this paper, we study how to achieve energy-aware service provisioning in a multi-domain EON, where the optoelectronic regenerators only exist in border nodes. We consider dynamic lightpath requests and propose two algorithms, namely, the greedy regenerator allocation (GRA) and the set-cover based regenerator allocation (STC), to realize the joint optimization of RMSA and regenerator allocation for improving the power efficiency. GRA tries to realize energy-aware service provisioning with a greedy manner, while STC leverages a set-cover based approach. We perform extensive simulations to evaluate the algorithms' performance in networks built with different regenerator placement strategies, and the results demonstrate that GRA and STC outperform the existing algorithm in terms of both blocking probability and power efficiency.

The rest of the paper is organized as follows. Section II formulates the problem of energy-aware service provisioning in multi-domain EONs. In Section III, the proposed algorithms are described in detail. We present the simulation results in Section IV, and finally, Section V summarizes the paper.

## II. PROBLEM FORMULATION

### A. Network Model

We use a set of graphs  $\mathbf{G} = \{G^i(V^i, E^i), i \in [1, N_{md}]\}$  to denote the topology of a multi-domain EON that has  $N_{md}$  domains, where  $V^i$  and  $E^i$  represent the sets of nodes and fiber links in the  $i$ -th domain, respectively. The border nodes in  $V^i$  are denoted as  $V_b^i$ , and we have  $V_b^i \subset V^i$ . We assume that only the border nodes in  $\bigcup_{i=1}^{N_{md}} V_b^i$  can be regeneration sites and the total number of regenerators in the multi-domain EON is fixed as  $N_{rg}$ . For any two directly connected domains  $G^i$  and  $G^j$ , the inter-domain links form a subset of  $V_b^i \times V_b^j$ . We assume that there are  $F$  frequency slots (FS') on each intra-/inter-domain link. Each FS has a bandwidth of 12.5 GHz and can provide a capacity of  $C_{FS} = 12.5$  Gb/s if its modulation format is BPSK [3]. We consider the case that there are four feasible modulation formats, *i.e.*, BPSK, QPSK, 8QAM and 16QAM, in the multi-domain EON.

For a multi-domain lightpath request  $LR(s, d, C)$ , the source and destination nodes reside in different domains and we need to perform RMSA and regenerator allocation to satisfy the capacity requirement  $C$ . Here, we define the modulation-level  $m$  of the modulation formats as  $m = 1, 2, 3$  and  $4$  for BPSK, QPSK, 8QAM and 16QAM, respectively. Hence, the number of spectrally-contiguous FS' that need to be assigned for  $LR$  is [14]

$$n = \lceil \frac{C}{m \cdot C_{FS}} \rceil + N_{gb}, \quad (1)$$

where  $N_{gb}$  is the number of FS' for the guard-band. Note that similar to the work in [11, 13], we also assume that the spectrum assignment and modulation selection of  $LR$  can be changed by a regenerator. Meanwhile, the maximum transmission reaches of BPSK, QPSK, 8QAM and 16QAM signals are assumed to be 5000 km, 2500 km, 1250 km and 625 km, respectively, based on the experimental results

reported in [3]. We also consider the power consumption of the regenerators (*i.e.*, bandwidth-variable transponders (BV-Ts)) and use the power model presented in [15]. Specifically, the power consumption of a BV-T is calculated as

$$P = (\alpha_m + P_0) \cdot n, \quad (2)$$

where  $\alpha_m$  is the dynamic power consumption per FS when using modulation-level  $m$ ,  $n$  is the number of FS' used, and  $P_0 = 91.3$  W is the static power consumption per FS. Here, according to [15], we have  $\alpha_1 = 21.1$  W,  $\alpha_2 = 42.1$  W,  $\alpha_3 = 63.2$  W and  $\alpha_4 = 84.2$  W.

### B. Energy-Aware Multi-Domain Service Provisioning

In this work, we consider the dynamic service provisioning in multi-domain EONs, where the lightpath requests can arrive and leave on-the-fly. For each request, we need to perform RMSA for it and make sure that the optical signal can be delivered across multiple domains with QoT guarantee. Therefore, we may divide the overall lightpath into a few transparent segments and insert a regenerator in between two adjacent segments. Note that since the regenerators only exist in border nodes, the regeneration site has to be selected under the location constraint. The RMSA solutions of different transparent segments are independent, but for each segment, the RMSA should satisfy the spectrum contiguous, continuous and non-overlapping constraints [14]. In the dynamic service provisioning, we try to minimize both the blocking probability and the power consumption of regenerators.

## III. PROPOSED ALGORITHMS

### A. Multi-Domain Provisioning Model

One important issue of multi-domain service provisioning is the mutual trust and service level agreements (SLAs) among the domains. Basically, due to the concern on intra-domain privacy, a domain operator may not want to disclose too much intra-domain information to the others. Therefore, in the multi-domain provisioning model, we assume that each domain only provides a high-level topology abstraction for calculating the RMSA and regenerator allocation of a multi-domain lightpath request  $LR(s, d, C)$ . Specifically, for serving  $LR$ , all the domains in  $\mathbf{G}$  contribute their own topology abstractions based on the current network status.

We assume that  $s$  locates in  $G^i$  (*i.e.*, source domain) and  $d$  is in  $G^j$  (*i.e.*, destination domain). The operator of  $G^i$  calculates a shortest path from  $s$  to each border node in  $V_b^i$ , while the operator of  $G^j$  figures out a shortest path from each border node in  $V_b^j$  to  $d$ . Each of the rest domains in  $\mathbf{G}$  provides a shortest path between every pair of its border nodes. Together with each shortest path, the operator also gives the information regarding the actual path length, number of hops, and available FS' on it. Note that since we assume that regenerators only exist in border nodes, an operator can only report a FS to be available when the FS is not occupied on any of the links on a shortest path. Then, with all the paths, we construct an auxiliary topology  $G^a(V^a, E^a)$ , where  $V^a = (\bigcup_{i=1}^{N_{md}} V_b^i) \cup \{s, d\}$  represents all the related nodes, and

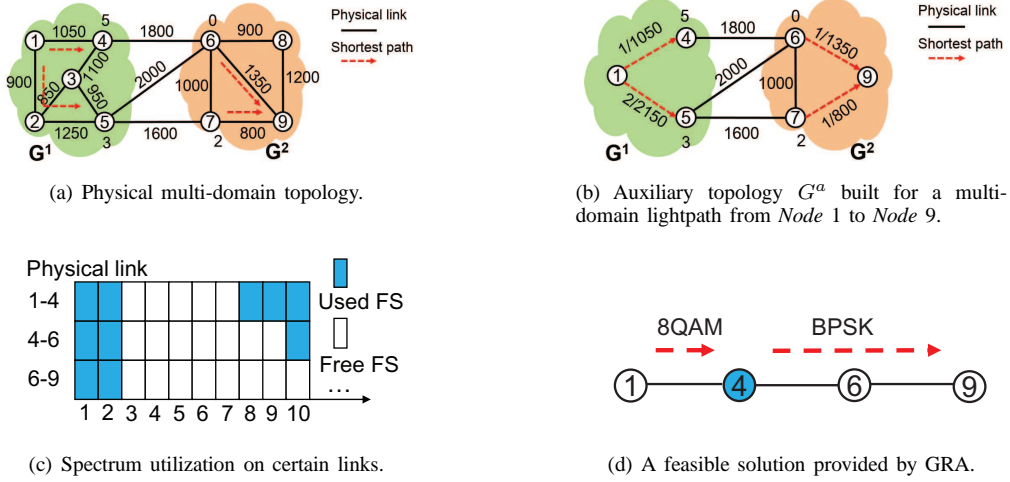


Fig. 1. Example on realizing multi-domain service provisioning with an auxiliary topology.

each virtual link  $e^a \in E^a$  corresponds to a shortest path or an inter-domain link. We obtain the provisioning scheme of  $LR$  (i.e., RMSA and regenerator allocation) based on  $G^a$ .

Fig. 1 shows an illustrative example on constructing the auxiliary topology. The physical topology of the multi-domain EON is in Fig. 1(a), which consists of two domains  $G^1$  and  $G^2$ . The fiber length in kilometers is labeled on each physical link, and the number of available regenerators is marked around each border node. Here, we assume that the source node is Node 1 and the destination node is Node 9. Then, the shortest paths in  $G^1$  are  $1 \rightarrow 4$  and  $1 \rightarrow 2 \rightarrow 5$ , and in  $G^2$ , we have  $6 \rightarrow 9$  and  $7 \rightarrow 9$ . By combining these paths with the inter-domain links, we obtain  $G^a$  as in Fig. 1(b), in which we label the actual number of hops and path length on each virtual link.

### B. Greedy Regenerator Allocation

We first try to achieve the energy-aware regenerator allocation in a greedy manner. *Algorithm 1* shows the detailed procedure of the greedy regenerator allocation (GRA). *Lines 1-4* are for initialization. The for-loop that covers *Lines 5-39* checks each path in  $\mathcal{P}_{s,d}$  and tries to obtain a feasible provisioning scheme with it. Specifically, for each  $p \in \mathcal{P}_{s,d}$ , we determine the RMSA and regenerator allocation for each transparent segment with  $u_1^a$  and  $u_2^a$ , which store the ingress and egress nodes of a transparent segment, respectively.

*Lines 6-7* initialize the procedure on  $p$ , and then the for-loop from *Line 8* to *Line 34* determines the provisioning scheme on it. Here, we define function  $len(u, v)$  to obtain the transmission distance of path segment  $u \rightarrow v$ . Basically, after initializing  $u_1^a$  as  $s$ , we check each node  $v^a \in p$  from the next node to  $s$  to  $d$ , and use *Lines 9-18* to determine whether a feasible RMSA exists for segment  $u_1^a \rightarrow v^a$ . If yes, *Lines 14-16* update  $u_2^a$  as  $v^a$ , store the RMSA (using first-fit spectrum assignment), and continue for the next  $v^a$ . Otherwise, a regenerator needs to be inserted in  $u_2^a$  for  $LR$ , since we already know that a feasible RMSA can be obtained for segment  $u_1^a \rightarrow u_2^a$ . As shown in *Lines 19-32*, if a regenerator is available on  $u_2^a$  for  $LR$ , we finalize the RMSA on segment

$u_1^a \rightarrow u_2^a$  and try to update  $u_1^a$  and  $u_2^a$  accordingly. If *Line 29* cannot be reached for whatever reason, *Line 33* breaks the loop since there is no feasible provisioning scheme on  $p$  for  $LR$ . On the other hand, if a feasible provisioning scheme can be obtained on  $p$ , *Lines 36-37* calculate its total power consumption on regenerators and store it in  $\Psi$ . Finally, *Lines 40-44* check whether feasible provisioning schemes exist for  $LR$ . If yes, we use the one that consumes the least power to serve  $LR$ . Otherwise, we mark  $LR$  as blocked.

We still use Fig. 1 to explain the operation of GRA. The spectrum utilization on certain physical links is shown in Fig. 1(c), and we consider a multi-domain request as  $LR(\text{Node 1, Node 9, } 75 \text{ Gb/s})$ . With the auxiliary topology in Fig. 1(b), we get the shortest path between *Nodes 1* and *9* as  $1 \rightarrow 4 \rightarrow 6 \rightarrow 9$ . Then, we first check segment  $1 \rightarrow 4$  and find that its length is 1050 km. Hence, the modulation format is selected as 8QAM. If we assume  $N_{gb} = 1$ , the number of FS' needed on segment  $1 \rightarrow 4$  can be obtained as  $n = 3$  with Eq. (1). Apparently, with the spectrum utilization in Fig. 1(c), we can allocate 3 spectrally-contiguous FS' to  $LR$  on segment  $1 \rightarrow 4$ . Hence, we update  $u_1^a$  and  $u_2^a$  as *Nodes 1* and *4*, respectively, and continue to check *Node 6*. The length of segment  $1 \rightarrow 6$  is 2850 km, which makes BPSK the only feasible modulation format, and we need to allocate 7 spectrally-contiguous FS' this time. However, the spectrum resource is insufficient, and we have to insert a regenerator in  $u_2^a$ , which is *Node 4*. By repeating the similar procedure, we get the feasible provisioning scheme for  $LR$  as in Fig. 1(d).

### C. Set-Cover based Regenerator Allocation

The energy-aware regenerator allocation can also be realized with a set-cover based approach by leveraging the weighted set-cover problem [16]. For a multi-domain lightpath request  $LR(s, d, C)$ , we still calculate  $K$  shortest paths in the auxiliary graph  $G^a$ . Then, on a path  $p \in \mathcal{P}_{s,d}$ , we get  $s$ ,  $d$  and all the intermediate nodes that have spare regenerator(s), and store them in node set  $\Lambda$ . Then, for each segment  $sg$  between a node pair in  $\Lambda$ , we check its length, determine possible RMSA(s) on

---

**Algorithm 1: Greedy Regenerator Allocation (GRA)**

---

**Input** :  $LR(s, d, C)$ ,  $\mathbf{G} = \{G^i(V^i, E^i)\}$ .

- 1 construct the auxiliary topology  $G^a(V^a, E^a)$  for  $LR$ ;
- 2 calculate  $K$  shortest paths for  $s \rightarrow d$  in  $G^a$ ;
- 3 store the paths in  $\mathcal{P}_{s,d}$ ;
- 4  $\Psi = \emptyset$ ;
- 5 **for each path**  $p \in \mathcal{P}_{s,d}$  **do**
- 6     set transparent distance  $D_{tp} = 0$ ;
- 7      $u_1^a = s$ ,  $u_2^a = s$ ;
- 8     **for each**  $v^a \in p$  **from the next node to  $s$  to  $d$**  **do**
- 9          $D_{tp} = \text{len}(u_1^a, v^a)$ ;
- 10        **if**  $D_{tp} \leq 5000$  **then**
- 11            get  $m$  as the modulation-level for segment  $u_1^a \rightarrow v^a$  based on  $D_{tp}$ ;
- 12            get  $n$  as the number of FS' needed on segment  $u_1^a \rightarrow v^a$  with Eq. (1);
- 13            **if**  $n$  spectrally-contiguous FS' are available on segment  $u_1^a \rightarrow v^a$  **then**
- 14                 $u_2^a = v^a$ ;
- 15                store RMSA on segment  $u_1^a \rightarrow u_2^a$ ;
- 16                **continue**;
- 17            **end**
- 18        **end**
- 19        **if**  $u_2^a$  has regenerator(s) **then**
- 20            place a regenerator in  $u_2^a$  for  $LR$ ;
- 21            finalize RMSA on segment  $u_1^a \rightarrow u_2^a$ ;
- 22             $u_1^a = u_2^a$ ,  $D_{tp} = \text{len}(u_1^a, v^a)$ ;
- 23            **if**  $D_{tp} \leq 5000$  **then**
- 24                get  $m$  as the modulation-level for segment  $u_1^a \rightarrow v^a$  based on  $D_{tp}$ ;
- 25                get  $n$  as the number of FS' needed on segment  $u_1^a \rightarrow v^a$  with Eq. (1);
- 26                **if**  $n$  spectrally-contiguous FS' are available on segment  $u_1^a \rightarrow v^a$  **then**
- 27                     $u_2^a = v^a$ ;
- 28                    store RMSA on segment  $u_1^a \rightarrow u_2^a$ ;
- 29                    **continue**;
- 30                **end**
- 31            **end**
- 32        **end**
- 33        **break**;
- 34     **end**
- 35     **if**  $u_2^a = d$  **then**
- 36         get the power consumption  $P_{tot}$  of  $LR$ ;
- 37         store the provisioning scheme and  $P_{tot}$  in  $\Psi$ ;
- 38     **end**
- 39 **end**
- 40 **if**  $\Psi = \emptyset$  **then**
- 41     mark  $LR$  as blocked;
- 42 **else**
- 43     use provisioning scheme in  $\Psi$  with the smallest  $P_{tot}$  to serve  $LR$ ;
- 44 **end**

---

it, and store the RMSA(s) (using first-fit spectrum assignment) in solution set  $\Phi$ . For instance, segment 4 $\rightarrow$ 6 $\rightarrow$ 9 in Fig. 1(b) has a length of 3150 km, which means that it can only support BPSK. Since it also has enough FS' to carry 75 Gb/s capacity for  $LR$ (Node 1, Node 9, 75 Gb/s) when using BPSK, we store the corresponding RMSA on segment 4 $\rightarrow$ 6 $\rightarrow$ 9 in  $\Phi$ . After checking all the segments on  $p$ , we assign a weight to each RMSA in  $\Phi$  to consider its spectrum usage and power consumption jointly.

$$w(sg) = \beta \cdot \text{hops}(sg) \cdot n + \gamma \cdot P(sg), \quad (3)$$

where  $sg$  is the corresponding segment on  $p$ ,  $\text{hops}(sg)$  returns the hop-count of  $sg$  in the auxiliary topology  $G^a$ ,  $n$  is the number of FS' needed by the RMSA (calculated with Eq. (1)),  $P(sg)$  obtains the power consumption of the RMSA with Eq. (2), and  $\beta$  and  $\gamma$  are the coefficients for normalization. Then, the energy-aware regenerator allocation for  $LR$  on  $p$  can be transformed into the weighted set-cover problem that tries to find the minimum-weighted cover (*i.e.*, a subset of  $\Phi$ ) whose elements have their union cover all the virtual links in  $p$ .

Algorithm 2 shows the detailed procedure of the proposed set-cover based regenerator allocation (STC). Lines 1-4 are for initialization. For each  $p \in \mathcal{P}_{s,d}$ , we use Lines 6-12 to build the RMSA set  $\Phi$ . Then, as shown in Line 13, the feasible provisioning scheme on  $p$  is obtained by finding the minimum-weighted cover in  $\Phi$ . Note that the optimization version of weighted set-cover is a  $\mathcal{NP}$ -hard problem in general [16]. Nevertheless, due to the scheme we used for building the auxiliary topology  $G^a$ , the scale of our problem is reasonably small and hence we can find the minimum-weighted cover quickly with either the exact integer linear programming (ILP) approach or a time-efficient heuristic [16]. For example, if we consider a relatively long lightpath that goes across four domains,  $\Lambda$  will include eight nodes at most. Then, in the worst case, we only need to check 28 segments to build  $\Phi$ .

#### IV. PERFORMANCE EVALUATION

We use the multi-domain topology in Fig. 2, which consists of five domains, to evaluate the performance of the proposed algorithms. The dynamic lightpath requests are generated with the Poisson traffic model, *i.e.*, requests come in according to the Poisson process with an average arrival rate of  $\lambda$  and their holding time follows a negative exponential distribution with an average of  $\frac{1}{\mu}$ . Hence, we can quantify the traffic load with  $\frac{\lambda}{\mu}$  in Erlangs. The source and destination nodes of each multi-domain lightpath request are randomly selected, and their capacity requirements are uniformly distributed within [12.5, 500] Gb/s. On each link in the topology, either an intra-domain or inter-domain one, there are  $F = 358$  FS', which correspond to 4.475 THz bandwidth in the C-band.

##### A. Regenerator Placement Strategies

The total number of regenerators is fixed as  $N_{rg}$  regenerator in the multi-domain EON. Here, in order to investigate the impact of regenerator distribution, we consider two regenerator placement strategies, *i.e.*, the even distribution strategy (EDS) and the topology-aware strategy (TAS). In EDS, we assign

---

**Algorithm 2: Set-Cover based Regenerator Allocation (STC)**


---

**Input** :  $LR(s, d, C)$ ,  $\mathbf{G} = \{G^i(V^i, E^i)\}$ .

- 1 construct the auxiliary topology  $G^a(V^a, E^a)$  for  $LR$ ;
- 2 calculate  $K$  shortest paths for  $s \rightarrow d$  in  $G^a$ ;
- 3 store the paths in  $\mathcal{P}_{s,d}$ ;
- 4  $\Psi = \emptyset$ ;
- 5 **for** each path  $p \in \mathcal{P}_{s,d}$  **do**
- 6      $\Lambda = \emptyset$ ,  $\Phi = \emptyset$ ;
- 7     form  $\Lambda$  to include  $s$ ,  $d$  and possible intermediate regeneration sites on  $p$ ;
- 8     **for** each segment  $sg$  between a node pair in  $\Lambda$  **do**
- 9         obtain all the possible RMSAs on  $sg$ ;
- 10         assign weights to the RMSAs with Eq. (3);
- 11         store the RMSAs and their weights in  $\Phi$ ;
- 12     **end**
- 13     try to find the minimum-weighted cover in  $\Phi$ ;
- 14     **if** the minimum-weighted cover can be found **then**
- 15         get the power consumption  $P_{tot}$  of  $LR$ ;
- 16         store the provisioning scheme and  $P_{tot}$  in  $\Psi$ ;
- 17     **end**
- 18 **end**
- 19 **if**  $\Psi = \emptyset$  **then**
- 20     mark  $LR$  as blocked;
- 21 **else**
- 22     use provisioning scheme in  $\Psi$  with the smallest  $P_{tot}$  to serve  $LR$ ;
- 23 **end**

---

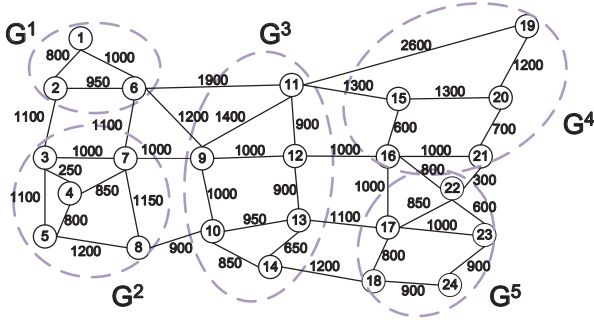


Fig. 2. Multi-domain EON topology (fiber lengths marked in kilometers).

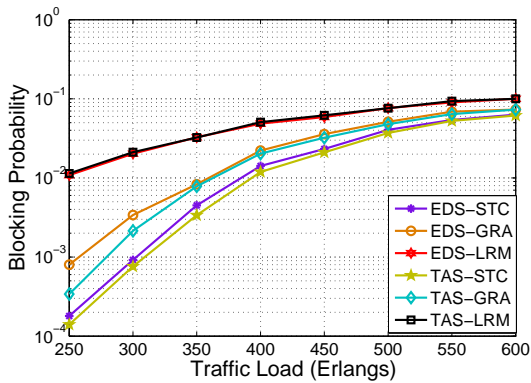


Fig. 3. Results on blocking probability with  $N_{rg} = 180$ .

TABLE I  
AVERAGE POWER EFFICIENCY ((Gb/s)/W) WITH  $N_{rg} = 180$ .

| Traffic Load (Erlangs) | EDS   |       |       | TAS   |       |       |
|------------------------|-------|-------|-------|-------|-------|-------|
|                        | LRM   | GRA   | STC   | LRM   | GRA   | STC   |
| 250                    | 0.082 | 0.110 | 0.114 | 0.082 | 0.110 | 0.114 |
| 300                    | 0.085 | 0.108 | 0.111 | 0.085 | 0.108 | 0.111 |
| 350                    | 0.088 | 0.105 | 0.109 | 0.088 | 0.105 | 0.108 |
| 400                    | 0.090 | 0.104 | 0.106 | 0.091 | 0.104 | 0.106 |
| 450                    | 0.093 | 0.106 | 0.106 | 0.093 | 0.105 | 0.106 |
| 500                    | 0.094 | 0.104 | 0.105 | 0.094 | 0.103 | 0.105 |
| 550                    | 0.097 | 0.105 | 0.108 | 0.098 | 0.104 | 0.106 |
| 600                    | 0.098 | 0.105 | 0.106 | 0.099 | 0.105 | 0.107 |

the same number of regenerators on every border node in the topology. TAS considers the degree of a border node when assigning regenerators to it. Specifically, if we assume that the set of border nodes is  $V_b = \bigcup_{i=1}^{N_{md}} V_b^i$  and  $deg(v)$  returns the degree of a border node  $v$ , then the number of regenerators to be assigned on border node  $v$  is  $\lfloor N_{rg} \cdot \frac{deg(v)}{\sum_{u \in V_b} deg(u)} \rfloor$ .

### B. Simulation Results

In the simulations, we use the LARA-M algorithm (LRM) developed in [13] as the benchmark, since it performed the best in [13]. We first fix the total number of regenerators as  $N_{rg} = 180$  and compare the algorithms in terms of request blocking probability and power efficiency. Here, both regenerator placement strategies are considered, and we name the simulation schemes with the combination of regenerator placement strategies and service provisioning algorithms. For instance, if we simulate STC in the multi-domain EON that uses EDS to place the regenerators, the name is EDS-STC.

Fig. 3 shows the results on blocking probability, which indicate that our proposed algorithms, *i.e.*, GRA and STC, always provide lower blocking probability than the benchmark (*i.e.*, LRM) no matter which regenerator placement strategy is used. This is because our algorithms are designed to utilize the limited regenerators more efficiently, while LRM only tries to balance the spectrum utilization, which may use up the regenerators quickly. We also observe that STC outperforms GRA in terms of blocking probability, and the reason is that STC considers spectral efficiency together with power consumption. When comparing the networks built with different regenerator placement strategies, we find that the results are close and for the same algorithm, the TAS-based scheme provides slightly lower blocking probability than the EDS-based one.

Table. I shows the results on average power efficiency in (Gb/s)/W, (*i.e.*, the ratio of total provisioned capacity to total power consumption). Again, GRA and STC achieve higher power efficiency than LRM, which verifies that by allocating regenerators only when they have to be used, GRA and STC can achieve significant power-saving. It is interesting to notice that the average power efficiency of LRM actually increases with the traffic load. We believe this phenomenon can be explained as follows. Since LRM only tries to balance the traffic load in the network, it may use a lot of regenerators even when the traffic load is relatively low. When the traffic load increases, the regenerators will be used up and this pushes

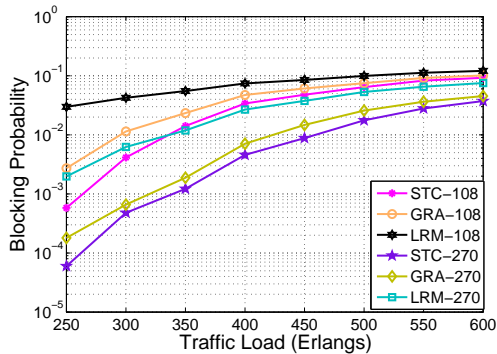


Fig. 4. Results on blocking probability with TAS.

LRM to serve requests without regenerators, which in turn improves the power efficiency. The results in Table I also indicate that STC is slightly more power efficient than GRA.

TABLE II  
AVERAGE POWER EFFICIENCY ((GB/s)/W) WITH TAS.

| Traffic Load (Erlangs) | $N_{rg} = 108$ |       |       | $N_{rg} = 270$ |       |       |
|------------------------|----------------|-------|-------|----------------|-------|-------|
|                        | LRM            | GRA   | STC   | LRM            | GRA   | STC   |
| 250                    | 0.093          | 0.110 | 0.114 | 0.073          | 0.110 | 0.114 |
| 300                    | 0.097          | 0.108 | 0.111 | 0.076          | 0.107 | 0.111 |
| 350                    | 0.099          | 0.107 | 0.110 | 0.079          | 0.105 | 0.109 |
| 400                    | 0.101          | 0.108 | 0.109 | 0.081          | 0.102 | 0.105 |
| 450                    | 0.105          | 0.110 | 0.111 | 0.084          | 0.102 | 0.104 |
| 500                    | 0.106          | 0.109 | 0.111 | 0.085          | 0.099 | 0.101 |
| 550                    | 0.109          | 0.112 | 0.113 | 0.087          | 0.099 | 0.101 |
| 600                    | 0.109          | 0.112 | 0.115 | 0.089          | 0.100 | 0.101 |

We then change the total number of regenerators to  $N_{rg} = 108$  and  $N_{rg} = 270$  and perform more simulations. As the regenerator placement strategies only affect the algorithms' performance slightly, we only simulate the TAS-based schemes. Fig. 4 shows the simulation results on blocking probability, which follow the similar trends as those in Fig. 3. Moreover, it can be seen that the blocking probability can be reduced significantly when we increase  $N_{rg}$ . This observation suggests that in the multi-domain EON, the major effect to cause request blocking is actually the shortage of regenerators, but not the spectrum insufficiency. Hence, for the service provisioning in such a multi-domain EON, people should pay more attention to the regenerator allocation as we do in this work.

In Table. II, we can see that for GRA and STC, when the traffic load is below 350 Erlangs, their power efficiencies stay almost unchanged for  $N_{rg} = 108$  and  $N_{rg} = 270$ . This is because in principle, GRA and STC only allocate regenerators when they are truly necessary, and when the traffic load is relatively low, the spectrum resources in the network are abundant and the chance that a regenerator is needed for spectrum conversion is slight. Therefore, GRA and STC do not increase their regenerator usages even when more regenerators are provided. In contrast, when we increase  $N_{rg}$  from 108 to 270, the power efficiency of LRM drops significantly even when the traffic load is below 350 Erlangs. When the traffic load is increased beyond 350 Erlangs, the power efficiencies of GRA and STC also drop with a larger  $N_{rg}$ , due to the fact that more regenerators have to be used to accommodate the increased traffic load.

## V. CONCLUSION

This work studied how to achieve energy-aware service provisioning in a multi-domain EON. We proposed two algorithms, namely, GRA and STC, to realize the joint optimization of RMSA and regenerator allocation for improving the power efficiency. The proposed algorithms were evaluated with extensive simulations and the results demonstrated that GRA and STC outperformed the existing algorithm for energy-aware multi-domain service provisioning, and STC achieved the best provisioning performance in terms of both blocking probability and power efficiency.

## ACKNOWLEDGMENTS

This work was supported in part by NSFC Project 61371117, Fundamental Research Funds for the Central Universities (WK2100060010), Natural Science Research Project for Universities in Anhui (KJ2014ZD38), and Strategic Priority Research Program of the CAS (XDA06011202).

## REFERENCES

- [1] O. Gerstel, M. Jinno, A. Lord, and S. J. B. Yoo, "Elastic optical networking: a new dawn for the optical layer?" *IEEE Commun. Mag.*, vol. 50, pp. S12–S20, Feb. 2012.
- [2] Z. Zhu *et al.*, "Demonstration of cooperative resource allocation in an OpenFlow-controlled multidomain and multinational SD-EON testbed," *J. Lightw. Technol.*, vol. 33, pp. 1508–1514, Apr. 2015.
- [3] A. Bocoï *et al.*, "Reach-dependent capacity in optical networks enabled by OFDM," in *Proc. of OFC 2009*, pp. 1–3, Mar. 2009.
- [4] B. Kozićki *et al.*, "Distance-adaptive spectrum allocation in elastic optical path network (SLICE) with bit per symbol adjustment," in *Proc. of OFC 2010*, pp. 1–3, Mar. 2010.
- [5] Y. Xi and B. Ramamurthy, "Dynamic routing in translucent WDM optical networks," in *Proc. of ICC 2002*, vol. 5, pp. 2796–2802, Jun. 2002.
- [6] K. Manousakis, P. Kokkinos, K. Christodouloupoulos, and E. Varvarigos, "Joint online routing, wavelength assignment and regenerator allocation in translucent optical networks," *J. Lightw. Technol.*, vol. 28, pp. 1152–1163, Apr. 2010.
- [7] Z. Zhu *et al.*, "Energy-efficient translucent optical transport networks with mixed regenerator placement," *J. Lightw. Technol.*, vol. 30, pp. 3147–3156, Oct. 2012.
- [8] X. Chen, F. Ji, Y. Wu, and Z. Zhu, "Energy-efficient resilience in translucent optical networks with mixed regenerator placement," *J. Opt. Commun. Netw.*, vol. 5, pp. 741–750, Jul. 2013.
- [9] A. Coiro, M. Listanti, and F. Matera, "Energy-efficient routing and wavelength assignment in translucent optical networks," *J. Opt. Commun. Netw.*, vol. 6, pp. 843–857, Oct. 2014.
- [10] M. Klinkowski, "On the effect of regenerator placement on spectrum usage in translucent elastic optical networks," in *Proc. of ICTON 2012*, pp. 1–6, Jul. 2012.
- [11] I. Cerutti *et al.*, "Trading regeneration and spectrum utilization in code-rate adaptive flexi-grid networks," *J. Lightw. Technol.*, vol. 32, pp. 4496–4503, Dec. 2014.
- [12] A. Fallahpour, H. Beyranvand, S. Nezamalhosseini, and J. Salehi, "Energy efficient routing and spectrum assignment with regenerator placement in elastic optical networks," *J. Lightw. Technol.*, vol. 32, pp. 2019–2027, May 2014.
- [13] Y. Song and F. Kuipers, "Impairment-aware routing in translucent spectrum-sliced elastic optical path networks," in *Proc. of NOC 2012*, pp. 1–6, Jun. 2012.
- [14] Z. Zhu, W. Lu, L. Zhang, and N. Ansari, "Dynamic service provisioning in elastic optical networks with hybrid single-/multi-path routing," *J. Lightw. Technol.*, vol. 31, pp. 15–22, Jan. 2013.
- [15] J. Lopez *et al.*, "On the energy efficiency of survivable optical transport networks with flexible-grid," in *Proc. of ECOC 2012*, pp. 1–3, Sept. 2012.
- [16] V. Vazirani, *Approximation Algorithms*. Springer-Verlag, May 2001.